Biosensors and Bioelectronics 25 (2010) 1193–1198

Contents lists available at ScienceDirect

Biosensors and Bioelectronics

journal homepage: www.elsevier.com/locate/bios

Development of microcantilever-based biosensor array to detect Angiopoietin-1, a marker of tumor angiogenesis☆

Carlo Ricciardi[a,*], Sonia Fiorilli[a], Stefano Bianco[a], Giancarlo Canavese[a], Riccardo Castagna[a], Ivan Ferrante[a], Gabriella Digregorio[a], Simone Luigi Marasso[a], Lucia Napione[b], Federico Bussolino[b]

[a] LATEMAR – Politecnico di Torino, Dipartimento di Scienza dei Materiali ed Ingegneria Chimica, Corso Duca degli Abruzzi 24, I-10129 Torino, Italy
[b] Department of Oncological Sciences, Institute for Cancer Research and Treatment, University of Torino, 10060 Candiolo, TO, Italy

ARTICLE INFO

Article history:
Received 28 July 2009
Received in revised form 2 October 2009
Accepted 8 October 2009
Available online 4 November 2009

Keywords:
Microcantilever
Angiogenesis
Protein detection
Precision
Specificity

ABSTRACT

Microcantilever biosensors have been proposed in the last years as very sensitive mass detectors, but few works focused on the precision and specificity of such tools. We measured the repeatability and reproducibility of our cantilever-based system, proponing the combination of results coming from both the first and second mode of vibration. Then, we optimized two biodesigns (a receptor-based and an antibody-based) to the detection of Angiopoietin-1, a possible marker in tumor progression. The reported results show that our microcantilever-based system can detect Angiopoietin-1 masses of the order of few hundreds of picograms with less than 0.5% of relative uncertainty. We showed that the evaluation of the protein surface density (number of molecules per cm^2) could reveal interesting features concerning the multimerization state of the targeted protein. We also performed negative controls (dipping the sample in PBS without proteins) and specificity tests (dipping the sample in PBS with a "false" antigen). The related frequency shifts coming from non-specific interactions were found to be at least one order of magnitude lower than typical variations due to specific protein binding. Thanks to its fine precision and optimal specificity, our microcantilever-based system can be successfully applied as a quantitative tool for systems biology studies such as the comprehension of angiogenic machinery and cancer progression.

1. Introduction

Proteomics opens new perspectives in many research areas of life sciences. In particular, in the field of medicine, proteomics activities might accelerate the discovery of new drug targets and protein disease markers useful for *in vitro* diagnostics (Vitzthum et al., 2005). This will lead to new pharmaceutical treatment opportunities and to reliable diagnostic information, which is essential for choosing the appropriate therapy. Besides providing reliable information about a person's condition and supporting therapeutic approach, proteomics plays a fundamental role in basic research, especially for a better comprehension of disease mechanisms and evolution (Emmert-Buck et al., 2000). For instance, in order to accurately diagnose and closely monitor complex diseases, such as cancer, the quantitative detection of multiple proteins is necessary. Protein analysis techniques currently used can be generally divided into four different categories: (1) radioactive, chemiluminescent, or fluorescent reporting of antigen–antibody binding (Zhu et al., 2000); (2) time-of-flight mass spectroscopy (Davies et al., 1999); (3) electrophoresis separation (Heegaard and Kennedy, 1999); and (4) detection of changes in surface properties due to antigen–antibody binding (Dahint et al., 1999; Mullett et al., 1998; Nicholson et al., 1999). Despite the virtue of these approaches with respect to precise protein quantification, problems remain with respect to the need of labeled molecules, cost and time for the analysis. Therefore, the development of label-free biosensors for sensitive and specific detection of protein analytes still represents an open challenge.

In the last few years, there has been a growing interest of bio and immuno-sensors using functionalized micromachined cantilevers to detect the presence of specific compounds (Waggoner and Craighead, 2007). In general, microcantilevers (MCs) can operate either as surface stress sensor or as a microbalance. The former measures the deflection originated from the stress generated in binding of the target molecules to the receptors on the MC surfaces, while the latter is used to detect the mass of the entities anchored to the cantilever surface using the decrease in the resonant frequency.

☆ To be presented at the 1st Biosensing Technology Conference, Bristol, UK, 10–12 November 2009.

* Corresponding author. Tel.: +390110907383; fax: +390110907399.
E-mail address: carlo.ricciardi@polito.it (C. Ricciardi).

0956-5663/$ – see front matter © 2009 Elsevier B.V. All rights reserved.
doi:10.1016/j.bios.2009.10.006

In recent years, it has been demonstrated that this technique in static mode is suitable to detect a single base pair mismatch in DNA hybridization experiments (Fritz et al., 2000) as well as transcription factors (Huber et al., 2006), and prostate-specific antigen (PSA) at clinically relevant conditions and concentration (Wu et al., 2001), without amplification or labeling of the sample. In dynamic mode, vibrating cantilever beams have been used to detect ultrasmall masses, ranging from femtogram down to the attogram range (Waggoner and Craighead, 2007). Determination of a single virus particle was performed in vacuum (Gupta et al., 2004) and quantitative detection in clinical ranges of PSA and specific C-reactive protein (CRP) has been reported (Lee et al., 2004).

In this work, we present the development of a microcantilever-based biosensor suitable to perform quantitative and precise detection of specific proteins. We chose Angiopoietin-1 (Ang-1) as our target molecule representative of the wide range of angiogenic factors, whose expression level is largely investigated in different tumors. Angiogenesis – the process of new blood vessel growth – plays an essential role in the development of tissues in the vertebrate embryo, and is also involved in a wide variety of physiological and pathological conditions in adults, including wound repair, metabolic diseases, inflammation, cardiovascular disorders, and tumor progression. In particular, the system represented by the tyrosine kinase receptor Tie-2 and its primary activating ligand Ang-1 is crucial for angiogenesis and for vascular maintenance in the embryo and in the adult. We performed Ang-1 binding experiments by hybridization reaction both with a human recombinant protein Tie-2/Fc and with the anti-Ang-1 monoclonal antibody (Ab). We achieved measurements with relative uncertainty lower than 0.5%, thanks to the combination of results coming from both the first and second mode of vibration, and showed that the evaluation of the protein surface density (number of molecules per cm^2) could reveal interesting features concerning the multimerization state of Ang-1.

2. Materials and methods

2.1. Reagents

Recombinant Protein A and Protein G, purified from Bacillus and Streptococcus respectively, were from PIERCE. Human recombinant proteins Tie-2/Fc, Ang-1 and VEGF-A_{165} were obtained from R&D Systems; Tie-2/Fc and Ang-1 were provided as 6XHIS-tagged. The anti-Tie-2 (sc-324) polyclonal Ab was from Santa Cruz Biotechnology; the anti-Ang-1 (A0604) mAb was from Sigma; the anti-6XHIS (552565) mAb was from BD Pharmingen; goat anti-mouse IgG (H + L) HRP-conjugated Ab and goat anti-rabbit IgG Fc HRP-conjugated Ab were from CHEMICON International. Protein A Sepharose CL-4B, Protein G Sepharose 4 Fast Flow, and 3,3′,5,5′-tetramethylbenzidine (TMB) were purchased from GE Healthcare Bio-Sciences. Dulbecco's Phosphate-Buffered Saline (PBS; BE17-512F) was procured from BioWhittaker/Cambrex.

3-Aminopropyltriehoxysilane (APTES, anhydrous, 99%, Aldrich), glutaraldehyde (GA, 25%, v/v, water solution) and toluene (anhydrous, 99.8%, Aldrich) were used without any further purification.

Sulphuric acid (95–97%, w/w) and hydrogen peroxide (30%, w/w) were also purchased from Sigma–Aldrich. Ortoboric acid and sodium chloride used to prepare borate buffer were ACS reagents (essay ≥99.5%) and were obtained from Sigma–Aldrich.

2.2. Design of in vitro biochemical assays preparatory for MC–protein binding experiments

Enzyme Linked ImmunoSorbent Assay (ELISA) experiments were specifically designed to verify silicon surface–protein binding specificity and immobilized protein activity; pull-down assay and immunoprecipitation (IP) experiments were used to establish the optimal experimental conditions for the Receptor–Ligand and the Ab–Antigen biodesigns, respectively (see Supplementary text and figures).

2.3. Microcantilever fabrication and measurement set-up

Arrays of microcantilevers (MCs) with dimensions of 400–800 μm in length, 50–120 μm in width and 2–3 μm in thickness were fabricated using a combination of surface and bulk micromachining process, as described in detail elsewhere (Canavese et al., 2007).

For the excitation of the MCs, a small piezoelectric disk (PI Ceramic) was used. A function generator (HP 33120A) produced a sinusoidal signal that was amplified and sent to the piezoelectric actuator, to give us the possibility to control the frequency of the oscillation. The actuator was linked to a holding cell, the cantilevers were attached to the actuator with double sided tape, and the cell was evacuated to a minimum pressure of 5×10^{-4} mbar by a series of a membrane and turbomolecular pump (MINI-Task System, Varian Inc. Vacuum Technologies). Cantilever vibrational characteristics were measured with the *optical lever* technique. The position of a focused laser beam reflected off the top side of the cantilever onto a position sensitive detector (PSD) was monitored. The current output of the PSD was amplified and converted into a voltage output, sent to a lock-in amplifier (EG&G 7260) for signal extraction and filtering, and stored to a personal computer, together with the stimulus signal for the function generator. The procedure was controlled in a LABVIEW® environment, while data were fitted with a Lorentzian curve and analyzed by software Origin™.

2.4. MC functionalization

A silicon oxide film on silicon MCs was grown by thermal oxidation at 1100 °C in O_2 atmosphere for 3 h. Before exposure to organosilanes, the SiO_2/Si MC were soaked into *piranha* solution (70% H_2SO_4:30% H_2O_2) for 15 min to remove organic contaminants, then rinsed with doubly distilled water and dried in a stream of nitrogen. Freshly cleaned MC were then incubated with 1% (v/v) solution of APTES in toluene at 60 °C for 10 min. Silane-coated MCs were rinsed several times with toluene and then dried in a stream of nitrogen. Freshly silanized-MCs were then incubated in a 1% GA solution (in borate buffer, 0.1 M; pH 8.8) for 1 h using an orbital shaker at 100 rpm. The relatively high pH ensures that mostly amino groups at MC surface are deprotonated (–NH_2) and thus able to react with aldehyde groups. After 15 min of incubation, 300 μL of a solution of sodiumcyanoboro hydride (5 M) in NaOH have been added to reduce the imine (–N=CH–) formed from the reaction between –NH_2 and –CHO moieties and thus to form a more stable bond. After incubation, MCs have been rinsed several times with doubly distilled water and dried in a stream of nitrogen.

Two biological binding experiments were then performed with the pre-activated MCs.

2.5. Protein binding experiments on functionalized MCs

2.5.1. "Receptor–Ligand" hybridization experiment

Functionalized MCs were soaked in a Protein A solution in PBS (50 μg/mL) for 2 h at room temperature using an orbital shaker. Afterward, MCs were washed in PBS (2×5 min and 2×10 min) to remove non-specifically bound proteins, and then in doubly distilled water (2×15 min) to remove possible salt residuals. After Protein A binding, 20 μL of Tie-2/Fc solution in PBS (2.5 μg/mL)

was dropped on MCs. The incubation of 2 h was performed at room temperature (RT) in a chamber with controlled humidity, to avoid evaporation of solution. After this, MCs were washed with PBS and doubly distilled water as reported before. Hybridization reaction with target receptor was carried out by dropping 20 μL of Ang-1 solution (25 μg/mL) in PBS; the incubation was of 2 h at RT in a chamber with controlled humidity. Washings were then performed as reported before.

2.5.2. "Ab–Antigen" hybridization experiment

Pre-activated MCs were incubated with a Protein G solution in PBS (50 μg/mL) for 2 h at RT using an orbital shaker. Afterward, MCs were washed (2 × 5 min and 2 × 10 min) in PBS—Tween 20 (0.05%) to remove non-specifically bound proteins, and then in doubly distilled water (2 × 15 min) to remove possible salt residuals. After Protein G binding, 5 μL of anti-Ang-1 Ab (A0604) solution in PBS (200 μg/mL) were dropped on MCs surface and the incubation performed for 2 h at RT under controlled humidity conditions. After this, MCs were washed with PBS and doubly distilled water as reported before. Hybridization reaction was carried out by dropping 20 μL of Ang-1 solution in PBS (25 μg/mL) and performing the incubation for 2 h at RT under controlled humidity conditions. After this, MCs were washed with PBS and doubly distilled water as reported before. Hybridization experiment on anti-Ang-1 Ab-bound MCs was also carried out with a VEGF-A_{165} antigen, non-specific for A0604 Ab, by using the same incubation conditions employed for Ang-1 hybridization reaction.

3. Results and discussion

The experiment consisted in characterizing the first and second flexural mode of different sized MCs in vacuum before and after protein immobilization. Using the following well-known equation, it is possible to link the shift of the eigenfrequency value Δf to the corresponding mass increment Δm:

$$\frac{\Delta f}{f_0} = -\frac{1}{2}\frac{\Delta m}{m_0} \quad (1)$$

where, f_0 is the resonant frequency and m_0 is the mass loading on the MC before binding. This direct relationship is applicable if the added mass is uniformly deposited on cantilever surface and if the beam spring constant k remains essentially constant after molecule binding. These requirements are commonly proofed in microcantilever-based biosensing, because the adsorbate properties such as thickness, stiffness and surface stress, have a neglecting influence on the vibrational characteristics of the Si resonator (Lu et al., 2005; Oliviero et al., 2008; Tamayo et al., 2006).

3.1. Preparatory measurements

First of all, we performed a critical run of measurements aimed at the evaluation of primary sources of uncertainty of the experimental set-up.

The first and second flexural mode of vibration in vacuum were monitored, while changing one by one the following parameters: vacuum level (4×10^{-2} to 8×10^{-4} mbar), laser spot on MC (3 positions between middle and free end), PSD angle with respect to laser reflected spot (33–40°), piezo-actuator applied tension (0.05–9 V), cantilever dimensions (3 different size MCs), operator (3 different researchers did optimize the same measurement). First flexural modes of vibration (M_1) were found in the range 4–8 kHz, while second modes (M_2) in the range 30–50 kHz. In such a way, we wanted to understand how the measurement uncertainty could be affected by the optimization of the experimental set-up. In particular, we wanted to compare the two modes in terms of precision (i.e. the variability of a measurement around its average value) rather than sensitivity. As a matter of fact, more than one research group has recently demonstrated the significant advantages in mass sensitivity when monitoring higher modes of vibration respect to the fundamental one (Waggoner and Craighead, 2007). However, such works usually focus just on the improved detector sensitivity (essentially given by the increasing of resonance curve Q-factor), while a careful analysis of repeatability and reproducibility of frequency measurement is needed, in our opinion, to corroborate such advantages.

To this purpose, 49 measurements of both M_1 and M_2 were collected in the above-mentioned conditions and 4 different histograms were created, using relative frequency shifts $\Delta f/f$ instead of absolute frequencies in order to compare different MCs and different vibration modes (see Fig. S3(a)–(d) in the Supplementary material). The standard deviation of the first mode resulted to be $\sigma_{M_1} = 2.7 \times 10^{-6}$, while the standard deviation of the second mode resulted to be $\sigma_{M_2} = 3.5 \times 10^{-6}$: therefore, M_2 uncertainty is evaluated to be roughly 30% greater than M_1 one. Furthermore, the range (i.e. the difference between the highest and lowest values) of the first set is half of the second: 1.3×10^{-5} versus 2.6×10^{-5}. Then, although both distributions are characterized by a significant and satisfying low uncertainty, we can deduce that, in our experimental set-up, measuring the second mode instead of the first one give a less precise result. If we consider all the data as a single distribution with 49 × 2 = 98 data (M_1M_2), we have $\sigma_{M_1M_2} = 3.1 \times 10^{-6}$, that is still larger than σ_{M_1}, and the range is clearly as large as M_2: 2.6×10^{-5}. On the contrary, if we calculate the arithmetic mean of the two modes as $M_{12} = (M_1 + M_2)/2$, the related distribution is characterized by the lowest standard deviation $\sigma_{M_{12}} = 2.5 \times 10^{-6}$, and the range is roughly the same as M_1: 1.4×10^{-5}.

Furthermore, the Chi-squared test shows that M_{12} distribution is the only one that follows a Gaussian distribution. We merged the external bins of the 4 histograms to have at least 5 counts for each bin and then we calculated the reduced $\tilde{\chi}_0^2$, in order to easily compare distributions with different degrees of freedom (Taylor, 1997). The results are $\tilde{\chi}^2_{M_1} = 5.6$, $\tilde{\chi}^2_{M_2} = 8.4$, $\tilde{\chi}^2_{M_1M_2} = 8.1$, $\tilde{\chi}^2_{M_{12}} = 4.1$. With a confidence level (P-value) of 5% we can state that just M_{12} has a non-significant discrepancy with a Gaussian distribution since $P_d(\tilde{\chi}^2 \geq \tilde{\chi}^2_{M_{12}}) \geq 5$, while it is significant for M_1 since $1 \leq P_d(\tilde{\chi}^2 \geq \tilde{\chi}^2_{M_1}) < 5$, and highly significant for M_2 and M_1M_2 since $P_d(\tilde{\chi}^2 \geq \tilde{\chi}^2_{M_2}, \tilde{\chi}^2_{M_1M_2}) < 1$ (Taylor, 1997).

Preliminary results, not reported here, on third and fourth modes show a similar behavior. We can then argue that higher modes can reduce the repeatability and reproducibility of the frequency measurement, while mediating them with the fundamental one represents a suitable tool to easily obtain precise and normally distributed measurements.

The obtained standard deviation $\sigma_{M_{12}} = 2.5 \times 10^{-6}$ can represent the uncertainty of the detector, which is remarkably lower with respect to the uncertainty of the whole bio-experiment. We performed negative control experiments, in which the protein-immobilized MCs are dipped into PBS solution to evaluate the influence of non-specific adsorption/desorption on resonance curves. We found that typical relative frequency shifts after PBS dipping are of the order of $(\Delta f/f)_{PBS} = 1 \times 10^{-4}$ (see Table S1(c) in the Supplementary material): although this value is 50 times larger than $\sigma_{M_{12}}$, it is still one order of magnitude lower than typical variations due to protein binding (see Fig. S4 in the Supplementary material for an example of a negative control experiment). Since non-specific binding is often addressed as the major limit on ultimate cantilever-based sensitivity (Waggoner and Craighead, 2007), we will use $(\Delta f/f)_{PBS}$ as our *experimental limit of detection*: frequency variation below this limit was labeled as statistical fluctuation.

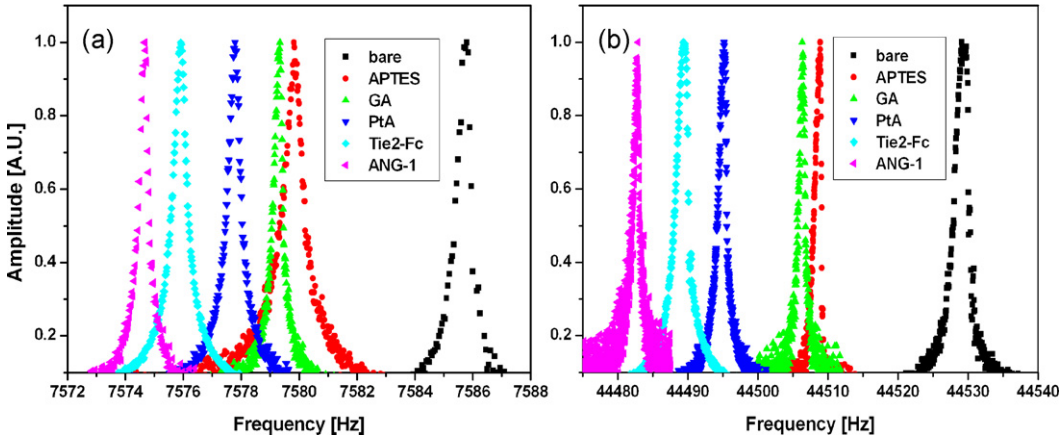

Fig. 1. Resonant curve for the Receptor–Ligand experiment: (a) first flexural mode, (b) second flexural mode. See text for further details. PtA is used as abbreviation of Protein A.

3.2. Receptor–Ligand experiment

As reported in Section 2, the Receptor–Ligand design is composed by 2 functionalization steps (APTES and GA), and 3 biomolecule binding steps (Protein A, Tie-2/Fc, Ang-1). Fig. 1 reports the resonance curves of first and second flexural mode of 28C4 after all the aforementioned steps, starting from the oxidized cantilever, denominated as "bare". The curves are normalized to 1 to facilitate the graphical comparison: in fact we frequently experienced variations in the intensity of the PSD signal, mainly due to the operator focusing of the laser beam. This fact also influences the Q-factor evaluation, that we found to vary in the range 5000–20,000, totally covering any possible trend linked to the variation of stiffness related to adsorption of soft materials like biomolecules. The figure shows that the receptor immobilization caused a frequency decrease of 1.88 Hz and 5.78 Hz, for M_1 and M_2 respectively; using Eq. (1), we obtain an average mass of $\Delta m_{12} = (0.19 \pm 0.06)$ ng. The uncertainty is calculated as half-deviation of the modes, $\sigma_{\Delta m_{12}} = (\Delta m_1 - \Delta m_2)/2$, because calculating standard deviation for few data can lead to an underestimation of the uncertainty.

Since we want to compare cantilever with different dimensions, we calculated the protein surface density (number of molecules per cm^2) as:

$$\delta = -\frac{2m_0\Delta f}{f_0}\frac{N_A}{MS} \quad (2)$$

where, N_A is the Avogadro constant, S the exposed surface of the beam, and M the molecular mass of the protein. For the receptor Tie-2/Fc (M = 165 kDa) we obtained an average value of $\delta_{12} = (0.47 \pm 0.15) \times 10^{12}$ molecules/cm^2. The response to following Ang-1 (M = 70 kDa) binding caused a negative shift of 1.24 Hz and 6.50 Hz, for M_1 and M_2 respectively, corresponding to an average mass increment of $\Delta m_{12} = (0.16 \pm 0.01)$ ng. Therefore, combining the two modes, we can not only detect a target mass as low as 160 pg (a value comparable with typical limit of detection of ELISA tests), but also easily give an uncertainty to such measurement: 10 pg, for this example. The calculated surface density resulted $\delta_{12} = (0.91 \pm 0.05) \times 10^{12}$ molecules/cm^2.

We can now consider each MC as a single instrument to measure the quantity δ_{12} and its related uncertainty $\sigma_{\delta_{12}}$ (given by half-deviation of the two modes); since we evidenced in Section 3.1 that such measurements are normally distributed, we can use the "weighted average" method to have the best estimation of the true value $\overline{\delta_{12}}$ (Taylor, 1997). Thanks to such method, the final value is closer to most precise measurements and intrinsically minimizes the contribution of data affected by largest uncertainty. From data listed in Table S1(a) and (b) (see Supplementary material), we obtained $\overline{\delta_{12}} = (0.45 \pm 0.02) \times 10^{12}$ and $\overline{\delta_{12}} = (0.91 \pm 0.05) \times 10^{12}$ molecules/cm^2, for Tie-2/Fc and Ang-1, respectively. The relative uncertainties of the entire sets are as small as 5%, confirming that our cantilever-based detection system can perform highly precise measurements.

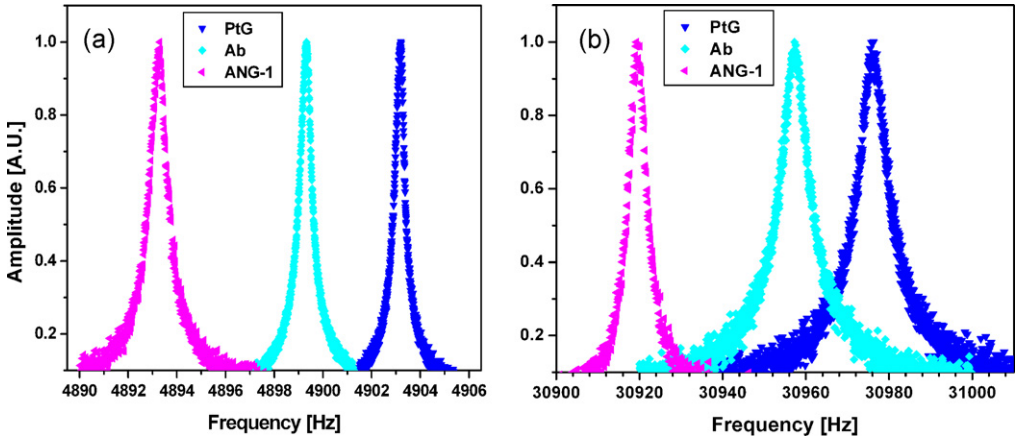

Fig. 2. Resonant curve for the Antibody–Antigen experiment: (a) first flexural mode, (b) second flexural mode. See text for further details. PtG is used as abbreviation of Protein G.

3.3. Ab–Antigen experiment

We here report about the Ab–Antigen design, where Protein A and Tie-2/Fc were substituted by Protein G and the anti-Ang-1 Ab, respectively. The chemical functionalization steps were not modified (APTES and GA).

Fig. 2 reports the resonance curves of first and second flexural mode of 33C3 after the three protein immobilization steps. It shows that the Ab immobilization caused a frequency decrease of 3.86 Hz and 18.86 Hz, for M_1 and M_2 respectively, corresponding to an average mass of $\Delta m_{12} = (0.23 \pm 0.03)$ ng. For the following Ang-1 binding we have a frequency decrease of 6.01 Hz and 37.69 Hz, for M_1 and M_2 respectively, corresponding to an average mass of $\Delta m_{12} = (0.411 \pm 0.001)$ ng. We then calculated the weighted average of the MC surface densities listed in Table S2(a) and (b) (see Supplementary material), obtaining $\overline{\delta_{12}} = (2.50 \pm 0.05) \times 10^{12}$ and $\overline{\delta_{12}} = (5.14 \pm 0.02) \times 10^{12}$ molecules/cm^2, for Ab and Ang-1, respectively. The evaluated Ab density is comparable with the theoretical maximum density estimated from the known size of an IgG molecule (23.5 nm × 2.5 nm), which is 1.7×10^{12} molecules/cm^2 (Gupta et al., 2006). The slightly higher value we obtained is probably related to the fact that cantilever surface with immobilized Ab is not nanometrically smooth. In fact, the functionalization and protein immobilization steps result in a three-dimensional corrugated surface and the related density of active sites is larger respect to that of a flat surface. The relative uncertainty of the entire set is smaller than 0.5%, indicating that the Ab–Antigen biodesign can perform the highest precise and accurate measurements.

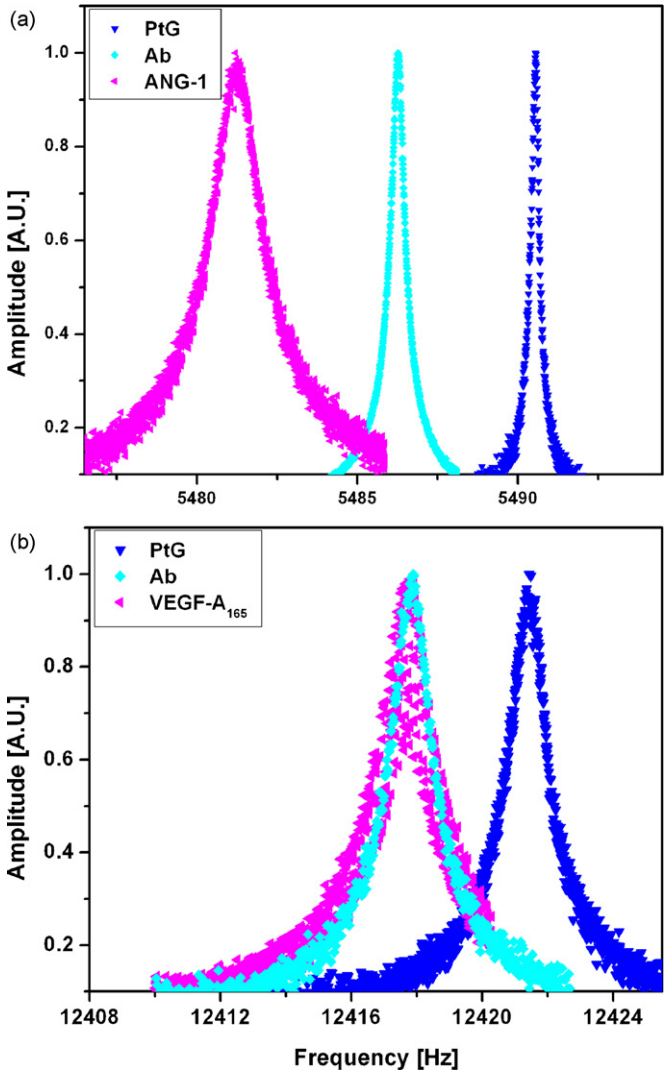

Fig. 3. Specificity test: (a) true antigen, Ang-1, (b) false antigen, VEGF-A_{165}. PtG is used as abbreviation of Protein G.

It is remarkable to note that this technique can also be used to investigate how many target molecules bound to each probe: from our data, the ratio of antigen/Ab surface density is 2.06 ± 0.05, perfectly consistent with the two binding sites of the Ab. Interestingly, we have found a similar value, 2.0 ± 0.2, also for ligand/receptor ratio, although the Tie-2/Fc receptor is known to have just one binding site (Barton et al., 2006). These results imply that Ang-1 is not present in its monomeric form; this suggestion is confirmed by other research groups that recently characterized its modular structure, evidencing the presence of variable-size multimers (Davis et al., 2003). From our measurements, the dimer seems to be the preferred immobilized conformation, but further studies are needed to deeply investigate the competitive kinetics of hybridization and the influence of washings. Anyhow, these results support that microcantilever biosensors can be successfully applied as a quantitative helpful tool in solving the multimeric state of a target molecule as well as the stoichiometry of protein–protein interaction.

We finally performed a specificity test, dipping five MCs in a solution containing a "false" antigen, VEGF-A_{165} (see Table S1(c) in the Supplementary material): in this way we wanted to check the system response due to the non-specific adsorption of proteins similar to the target molecule, Ang-1. The average relative frequency shift resulted $\overline{(\Delta f/f)_{VEGF}} = (-1.1 \pm 0.8) \times 10^{-5}$, lower than our experimental limit of detection (see subsection 3.1 and Supplementary text) and nearly two orders of magnitude lower than typical shifts due to specific recognition. Fig. 3 reports the graphical comparison between resonance curves of one cantilever dipped in Ang-1 solution (denominated "true" antigen) versus one dipped in VEGF-A_{165} solution ("false" antigen). The same relative scale on x-axis is used to better evidence the large difference in the frequency shift induced by protein adsorption.

4. Conclusions

We reported our successful experiments on the detection of Ang-1, a marker of tumor angiogenesis. We particularly focused on the precision and accuracy of our cantilever-based analysis, proponing the combination of results coming from both the first and second mode of vibration. A careful analysis of repeatability and reproducibility was performed as preparatory measurements. Two biodesigns were optimized and compared: Receptor–Ligand and Ab–Antigen. The latter gave the best results in terms of highest surface density and lowest uncertainty: Ang-1 masses of the order of few hundreds of picograms were detected with less than 0.5% of relative uncertainty. We showed that the evaluation of the protein surface density (number of molecules per cm^2) could reveal interesting features concerning the multimeric state of the targeted protein. We also performed negative controls (dipping the sample in PBS without proteins) and specificity tests (dipping the sample in PBS with a "false" antigen). The related frequency shifts (coming from non-specific interactions) were found to be at least one order of magnitude lower than typical variations due to specific protein binding.

Thanks to its fine precision and optimal specificity, our microcantilever-based system can be successfully applied as a quantitative tool for systems biology studies such as the comprehension of angiogenic machinery and cancer progression.

Acknowledgements

The authors are thankful for the financial support of MIUR (FIRB2003-LATEMAR, PRIN2005 and PRIN2007 grant) and Regione Piemonte (CIPE2004 grant). G.C. was supported by Fondazione CRT (Progetto Lagrange). This study was also supported by: Associazione Italiana per la Ricerca sul Cancro (AIRC); Ricerca industriale e competitiva 2006, grant PRESTO; Ricerca Tecnologie convergenti 2007, grant PHOENICS; Piattaforme tecnologiche per le biotecnologie, grant DRUIDI; Fondazione CRT – Torino; and 'Ministero della Salute' (Programma Ricerca Oncologica 2006, Ricerca Finalizzata 2006, 2007).

Appendix A. Supplementary data

Supplementary data associated with this article can be found, in the online version, at doi:10.1016/j.bios.2009.10.006.

References

Barton, W.A., Tzvetkova-Robev, D., Miranda, E.P., Kolev, M.V., Rajashankar, K.R., Himanen, J.P., Nikolov, D.B., 2006. Nat. Struct. Mol. Biol. 13, 524–532.
Canavese, G., Marasso, S.L., Quaglio, M., Cocuzza, M., Ricciardi, C., Pirri, C.F., 2007. J. Micromech. Microeng. 17, 1387–1393.
Dahint, R., Bender, F., Morhard, F., 1999. Anal. Chem. 71, 3150–3156.
Davies, H., Lomas, L., Austen, B., 1999. Biotechniques 27, 1258–1261.
Davis, S., Papadopoulos, N., Aldrich, T.H., Maisonpierre, P.C., Huang, T., Kovac, L., Xu, A., Leidich, R., Radziejewska, E., Rafique, A., Goldberg, J., Jain, V., Bailey, K., Karow, M., Fandl, J., Samuelsson, S.J., Ioffe, E., Rudge, J.S., Daly, T.J., Radziejewski, C., Yancopoulos, G.D., 2003. Nat. Struct. Biol. 10, 38–44.
Emmert-Buck, M.R., Strausberg, R.L., Krizman, D.B., Bonaldo, M.F., Bonner, R.F., Bostwick, D.G., Brown, M.R., Buetow, K.H., Chuaqui, R.F., Cole, K.A., Duray, P.H., Englert, C.R., Gillespie, J.W., Greenhut, S., Grouse, L., Hillier, L.W., Katz, K.S., Klausner, R.D., Kuznetzov, V., Lash, A.E., Lennon, G., Linehan, W.M., Liotta, L.A., Marra, M.A., Munson, P.J., Ornstein, D.K., Prabhu, V.V., Prange, C., Schuler, G.D., Soares, M.B., Tolstoshev, C.M., Vocke, C.D., Waterston, R.H., 2000. Am. J. Pathol. 156, 1109–1115.
Fritz, J., Baller, M.K., Lang, H.P., Rothuizen, H., Vettiger, P., Meyer, E., Güntherodt, H.-J., Gerber, C., Gimzewski, J.K., 2000. Science 288, 316–318.
Gupta, A.K., Nair, P.R., Akin, D., Ladisch, M.R., Broyles, S., Alam, M.A., Bashir, R., 2006. Proc. Natl. Acad. Sci. U.S.A. 103, 13362–13367.
Gupta, A., Akin, D., Bashir, R., 2004. Appl. Phys. Lett. 84, 1976–1978.
Heegaard, N.H., Kennedy, R.T., 1999. Electrophoresis 20, 3122–3133.
Huber, F., Hegner, M., Gerber, C., Güntherodt, H.J., Lang, H.P., 2006. Biosens. Bioelectron. 21, 1599–1605.
Lee, J.H., Yoon, K.H., Hwang, K.S., Park, J., Ahnc, S., Song Kima, T., 2004. Biosens. Bioelectron. 20, 269–275.
Lu, P., Lee, H.P., Lu, C., O'Shea, S.J., 2005. Phys. Rev. B 72, 085405.
Mullett, W., Lai, E.P., Yeung, J.M., 1998. Anal. Biochem. 258, 161–167.
Nicholson, S., Gallop, J.L., Law, P., Thomas, H., George, A.J., 1999. Lancet 353, 808.
Oliviero, G., Bergese, P., Canavese, G., Chiari, M., Colombi, P., Cretich, M., Damin, F., Fiorilli, S., Marasso, S.L., Ricciardi, C., Rivolo, P., Depero, L.E., 2008. Anal. Chim. Acta 630, 161–167.
Tamayo, J., Ramos, D., Mertens, J., Calleja, M., 2006. Appl. Phys. Lett. 89, 224104.
Taylor, J.R., 1997. An Introduction to Error Analysis: The Study of Uncertainties in Physical Measurements, second ed. University Science Books.
Vitzthum, F., Behrens, F., Leigh Anderson, N., Shaw, H.J., 2005. J. Proteome Res. 4, 1086–1097.
Waggoner, P.S., Craighead, H.G., 2007. Lab Chip 7, 1238–1255.
Wu, G., Datar, R.H., Hansen, K.M., Thundat, T., Cote, R.J., Majumdar, A., 2001. Nat. Biotech. 19, 856–860.
Zhu, H., Klemic, J.F., Chang, S., Bertone, P., Casamayor, A., Klemic, K.G., Smith, D., Gerstein, M., Reed, M.A., Snyder, M., 2000. Analysis of yeast protein kinases using protein chips. Nat. Genet. 26, 283–289.